Article

Biophotonic Effects of Low-Level Laser Therapy at Different Wavelengths for Potential Wound Healing

Tzu-Sen Yang [1,2,3,4,5,†], **Le-Thanh-Hang Nguyen** [1,6,†], **Yu-Cheng Hsiao** [1], **Li-Chern Pan** [1] and **Cheng-Jen Chang** [1,5,7,8,*]

1 Graduate Institute of Biomedical Optomechatronics, Taipei Medical University, Taipei 110, Taiwan
2 International Ph.D. Program in Biomedical Engineering, Taipei Medical University, Taipei 110, Taiwan
3 School of Dental Technology, Taipei Medical University, Taipei 110, Taiwan
4 Research Center of Biomedical Device, Taipei Medical University, Taipei 110, Taiwan
5 TMU Research Center of Cancer Translational Medicine, Taipei Medical University, Taipei 110, Taiwan
6 Faculty of Applied Sciences, Ton Duc Thang University, Ho Chi Minh City 700000, Vietnam
7 Department of Plastic Surgery, Taipei Medical University Hospital, Taipei 110, Taiwan
8 Department of Surgery, School of Medicine, College of Medicine, Taipei Medical University, Taipei 110, Taiwan
* Correspondence: chengjen@tmu.edu.tw
† These authors contributed equally to this work.

Abstract: Our objective was to assess the effect of low-level laser therapy (LLLT) administered using a diode laser on the growth processes of human fibroblast cells involved in wound healing. Initially, studies were conducted using a diode laser at wavelengths of 633, 520, and 450 nm with an irradiance of 3 mW/cm^2. The distance between the light source and culture plate was 3 cm. The mechanism(s) of action of the diode laser illumination on human fibroblast cells were studied by examining different wavelengths to determine the relevant light parameters for optimal treatment. In addition, the percentages of fibroblast-mediated procollagen and matrix metallopeptidase (MMP)-1, -2, and -9 production were compared. In the clinical study, the changes in basic fibroblast growth factor (bFGF), vascular endothelial growth factor (VEGF), and fibroblast collagen production were assessed in 60 patients with complicated wounds who received LLLT (633 nm). No statistically significant difference was observed between red light versus green and blue light in the viability analysis. In addition, the effects of LLLT on the cell cultures of fibroblast cells in vitro demonstrated a decrease in the relative expression of MMP-1, -2, and -9 while using light with a wavelength of 633 nm. In the clinical study, 633 nm diode laser LLLT at 2–8 J/cm^2 was administered to 60 patients with complicated wounds; all patients showed increased levels of bFGF and VEGF and the occurrence of collagen synthesis. Our studies demonstrated that LLLT might affect fibroblast cell growth processes involved in wound healing.

Keywords: low-level laser therapy; diode laser; fibroblast cells; matrix metallopeptidase; wound healing

1. Introduction

Low-level laser therapy (LLLT), also known as photobiomodulation (PBM), is a medical technique that stimulates cellular function, resulting in beneficial clinical effects. LLLT has two characteristics: LLLT is characterized by a biphasic dose response, namely, lower doses of light are often more beneficial than high doses, and a large number of parameters such as the wavelength, fluence, irradiance, illumination irradiation time, and timing of the applied light must be chosen for LLLT treatment [1]. For example, the primary defining factor is power with a range of 10^{-3}–10^{-1} W. Other significant parameters include an irradiance (power/area) of 10^{-2}–10 W/cm^2 and a dose or fluence (power × illumination irradiation time/area irradiated) of 10^{-2}–10^2 J/cm^2. Differences in the parameters used in

different studies complicate the meaningful comparisons. On the other hand, LLLT differs from other light-based treatments because it does not ablate and is not based on heating. In addition, LLLT differs from photodynamic therapy, which is based on the effect of light to excite exogenously delivered photosensitizers to produce toxic reactive oxygen species (ROS) [2].

Whelan et al. conducted in vitro and in vivo studies to assess the effects of hyperbaric oxygen and near-infrared (NIR) light therapy on wound healing using various wavelengths, power intensities, and energy density parameters of diode lasers to identify the conditions optimal for biostimulation [3]. These studies found that using diode laser LLLT for light therapy alone or in conjunction with hyperbaric oxygen significantly improves natural wound healing and quickly returns the patient to pre-injury or pre-illness levels. In a rodent model of mitochondrial poison-induced blindness, Whelan et al. demonstrated that NIR (670 nm, 4 J/cm^2) treatment heals poisoned neurons by stimulating cytochrome oxidase activity, protects against retinal damage, and improves retinal function recovery. Furthermore, it promotes retinal healing and improves visual function in adult nonhuman primates after high-intensity laser-induced retinal injury [4]. Neither experimental nor clinical studies have found evidence of retinal or optic nerve damage due to LLLT.

Furthermore, Whelan et al. conducted in vitro and in vivo studies using a variety of light-emitting diode (LED) wavelength, power intensity, and energy density parameters to identify conditions optimal for biostimulation. In later research, they demonstrated that NIR LED treatment heals poisoned neurons through the stimulation of cytochrome oxidase activity, which protects against retinal damage and improves the retinal function in a rodent model of mitochondrial poison-induced blindness; furthermore, it promotes retinal healing and improves visual function following high-intensity laser-induced retinal injury in adult non-human primates [3–5]. Moreover, Desmet et al. studied the use of NIR light treatment in various in vitro and in vivo models to determine the effect of NIR LED light treatment on physiologic and pathologic processes [6].

Wound healing is a complex interaction involving numerous cell types, cytokines, and mediators, and the extracellular matrix. It can be divided into three phases: The inflammatory phase, the proliferative phase, and the remodeling phase. Platelets, neutrophils, macrophages, and lymphocytes migrate to a wound during the inflammatory phase. The proliferative phase is characterized by an increase in fibroblasts and macrophages, as well as a decrease in the acute-phase reactants. Finally, during the remodeling phase, fibroblasts help to recreate the extracellular matrix and deposit collagen [7].

Human skin fibroblasts play a critical role in a range of wound repair processes. Increasing research has been dedicated to the possibility of using the LED and the laser to increase fibroblast activity and collagen synthesis further to obtain an economical and feasible procedure for wound repair without using costly and immobile light systems currently used for wound therapy. Because the fibroblast plays a crucial role in wound healing, most of the LLLT-related published studies have examined the effect of LLLT on fibroblast cell growth, locomotion, and collagen production. The experimental results have demonstrated that NIR LED light treatment stimulates mitochondrial oxidative metabolism in vitro and speeds up the cell and tissue repair in vivo [8–11].

Although a variety of photoreceptors are present in cells and tissues, light absorption can be divided into a green-blue band and a red–infrared band. LLLT with red to NIR light (630–1000 nm) accelerates wound healing, attenuates degeneration in the injured optic nerve, and improves recovery from ischemic injury. At the cellular level, low-energy photo illumination can have significant biological effects, such as cell proliferation and the release of growth factors [5,6,8–11]. A recent study showed that the red–infrared band had better wound-healing effects at the organism level than the green–blue band. In addition, a combination of the green–blue and red–infrared bands presented a better effect than the two bands alone [12].

Various studies have been conducted to improve the understanding of the effects of LLLT at the cellular level. Given that early research suggested laser-mediated improvement

in wound healing, more recent low-level laser studies have further focused on the effect of laser on cell growth processes involved in wound repair [7,13]. Thus, administering LLLT in the red to NIR range using a diode laser for PBM represents an innovative and non-invasive therapeutic approach for treating retinal injury and disease. We recently constructed a continuous-wave laser-induced forward transfer (CW-LIFT) system capable of controlling and precise depositing cells [14]. In addition, a single-cell NIR laser irradiation system (830 nm) and the image-based approaches were proposed for studying the modulatory effects in mitochondrial membrane potential ($\Delta\Psi m$), reactive oxygen species (ROS), and vesicle transport in single living human adipose mesenchymal stem cells (hADSCs). We found an increase in $\Delta\Psi m$, ROS, and vesicle transport in the irradiated-hADSCs at a fluence of 5 J/cm^2 [15]. In this study, we proposed the microscope objective-based LLLT illumination system, slightly modified from this CW-LIFT cell printing system, to assess the biophotonic effect of LLLT and investigate the effects of LLLT with three different wavelengths of 450 nm, 520 nm, and 633 nm diode lasers on fibroblast growth, matrix metalloproteinases (MMPs) levels, and the feasibility of its clinical application in wound healing.

2. Materials and Methods

2.1. Human Fibroblast Cells

Human fibroblast cells (HS 68) were prepared using the procedures reported by Zuk et al. [16]. First, the dermal tissue was finely minced, digested with 0.1% collagenase (Wako, Osaka, Japan), and vigorously shaken for 40 min at 37 °C in a 50 cm^3 centrifuge tube. To neutralize the added collagenase, an equal volume of Dulbecco's modified Eagle medium (DMEM) with 10% fetal bovine serum was added. The cell suspension was then centrifuged for 5 min at 1300 rpm (260 g). The cell pellet was then suspended, and the cells were counted using trypan blue dye before being plated in DMEM at a concentration of 1×10^6 cells per 100 mm^2 tissue culture plate. The cells were kept at 37 °C in 5% CO$_2$ [17]. The medium was changed every 3 days, and the nonadherent cells were discarded. The cells were passaged at a 1:3 ratio per week. In this study, only cells cultured for three passages were used.

The fibroblast cells were pelleted through centrifugation (1000 rpm) for 5 min, resuspended in Cell Applications Dermal Cells proliferation medium (Cell Applications, Inc., San Diego, CA, USA), and plated on fibronectin-coated T25 flasks. One week before LLLT, the fibroblast cells were subcultured using DMEM with 10% fetal bovine serum, 4 mM L-glutamine adjusted to contain 1.5 g/L sodium bicarbonate, and 4.5 g/L glucose (Cell Applications, Inc.) in each T80 (80 cm^2) culture flask under 5% CO$_2$ for 5 min at 37 °C. Then, the human fibroblast cells were neutralized using the same amount of Trypsin Neutralizing Solution (Cell Applications, Inc.) and counted using a hemocytometer.

The fibroblast cells were then plated on an attachment factor solution (Cell Applications, Inc.)-coated 24-well plate at a density of 2.5–3.5 $\times 10^4$ and maintained in 300 µL of supplemented DMEM culture medium with 1% FBS for 24 h to allow the cells attach to the bottom of the wells. On the day of LLLT, the fibroblast cells were washed with fresh PBS for 5 min and exposed to lights of different wavelengths (λ = 633, 520, and 450 nm). Diode laser illumination was performed at different wavelengths and compared with the control group, which was not illuminated. The fibroblast cells were incubated for 1 day, and cell viability was then determined by applying 30 µL of Alamar Blue—added aseptically—before and after illumination for 3 days. After diode laser illumination, morphological changes were observed using a light microscope and videotaped.

2.2. Low-Level Laser Illumination

The diode laser light was adjusted to emit light at wavelengths of 633, 520, and 450 nm for each experiment (Figure 1). The proposed laser illumination system consists of a wavelength of 450 nm, 520 nm, and 633 nm diode laser (PL450B, PL520, HL6333DG, Thorlabs, Newton, NJ, USA), respectively, laser-focusing optics (20× objective lens), an electrical

shutter, and a specimen holder attached to the *xyz*-axis steel stage. The objective-based LLLT illumination system has two advantages: The area of the laser influence zone can be adjusted by adjusting the distance between the objective lens and the sample, and the upright-placed objective lens can capture the corresponding sample image. Laser illumination projected a circular field of uniform light intensity. The emission was monitored using a Coherent Model 210 power meter before and after illumination. The mechanism(s) of action of low-level laser illumination on fibroblast cells were studied to determine the relevant light parameters of the dosimetry model for optimal cell proliferation [17]. Diode laser illumination was performed at different wavelengths and compared with the control group, which was not illuminated. Evaluated interventions to the cellular groups for illumination included (A) control (no LLLT), (B) 633 nm, (C) 520 nm, and (D) 450 nm. In this study, the distance from the exit of the CFI Super Plan Fluor ELWD $20\times/0.45$ NA objective (Nikon, Tokyo, Japan) to the culture plate is 3 cm. An illumination light source with an appropriate wavelength provides the energy to drive proliferative reactions without heat generation. The irradiance was maintained at 3 mW/cm^2.
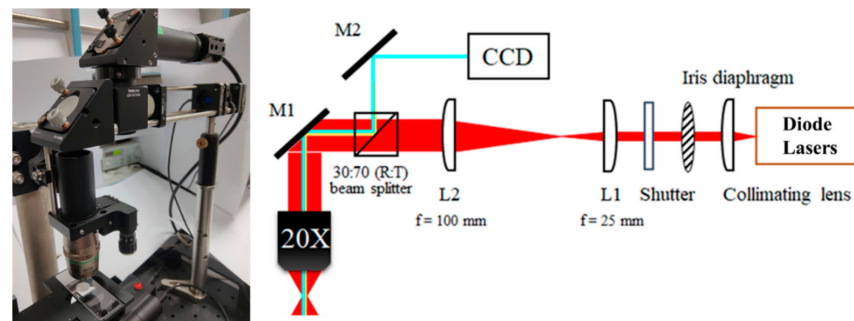

Figure 1. The experimental setup for the proposed LLLT illumination system consists of diode lasers at wavelengths of 450 nm, 520 nm, and 633 nm, respectively, laser-focusing optics ($20\times$ objective lens), an electrical shutter, and a specimen holder attached to the *xyz*-axis steel stage.

2.3. Assessment of Cell Viability

Twenty-four hours after LLLT, changes were observed using the light microscope. The CytoTox 96$^{\text{TM}}$ Assay (Promega Co., Madison, WI, USA) was used to assess the lactic dehydrogenase (LDH) percentage from fibroblast cells after diode laser illumination. The LDH released in culture supernatants was measured by converting tetrazolium salt into a red formazan product. The intensity of the color was proportional to the number of lysed cells. The visible absorbance was read at 490 nm using a ThermoMax microplate reader (Molecular Devices, Menlo Park, CA, USA). Cell viability is defined as [((test sample count) − (blank count))/((untreated control count) − (blank count))] × 100.

2.4. Real-Time Polymerase Chain Reaction and Enzyme-Linked Immunosorbent Assay

After LLLT, HS68 cells were incubated with serum-free DMEM. The cell culture medium was collected 24 h after LLLT, and matrix metallopeptidase (MMP)-1 and type-I procollagen production were quantified using a human MMP-1 ELISA kit (QIA55; Merck & Co., Inc., Whitehouse Station, NJ, USA) and a procollagen type-I C-peptide enzyme immunoassay kit (Thermo Fisher Scientific Inc., Waltham, MA, USA), respectively. Meanwhile, a collective review of cell proliferation and the real-time polymerase chain reaction (RT-PCR) for MMP-1, -2, and -9 were performed on an ABI 7500 machine with SYBR Premix Ex Tag (TaKaRa, Otsu, Japan). PCR conditions were as follows: 30-s hot start at 95 °C, followed by 34 cycles for 5 s at 95 °C and 34 s at 60 °C [18]. RT-PCR was performed three times for confirmation.

2.5. Clinical Study: Histological and Immunohistochemical Analysis

In total, 60 patients with chronic wounds (wound healing taking longer than 3 months) were chosen for LLLT from January 2014 to November 2016. Chronic wounds were located

on the trunk and limbs. After an institutional review board (IRB)-approved protocol of the Ministry of Health and Welfare in Taiwan (TS202-S002-E002), informed consent was obtained from the patient. LLLT was administered with a circular application of continuous diode laser illumination with 400 mW and irradiance of 3 mW/cm^2 at a wavelength of 633 nm, where the radius and area of the laser influence zone are 6.5 cm and 133 cm^2, respectively. The fluence used was 2–8 J/cm^2. Treatment was given twice a week, with a minimal interval of 3 days for 8 weeks. Skin biopsies were performed to investigate the mechanisms and biological responses before LLLT and 4 weeks after the wound healed. Sections of tissue samples were cut and placed on microscope slides. The Discovery XT automated immunohistochemistry stainer (Ventana Medical Systems, Inc., Tucson, AZ, USA) was used to stain the slides. We used the Ventana Chromo Map Kit (Ventana Medical Systems) for detection. The tissue sections were deparaffinized, and CC1 standard (pH 8.4 buffer contained Tris/borate/ethylenediaminetetraacetic acid) was used to retrieve the antigen. Inhibitor D (3% H$_2$O$_2$, endogenous peroxidase) was plugged in for 4 min at 37 °C [7,8,13,17]. The slides were incubated for 32 min at 37 °C with anti-collagen type 1 (Millipore, Billerica, MA, USA). The slides of tissue biopsy obtained from five sites of the healed wound were assessed through densitometric analysis of collagen by using image analysis software (Leica Qwin V3 and Veica Microsystems CMS GmbH, Wetzlar, Germany) on tissues stained with Masson's trichrome. This was measured at five places on one slide.

2.6. Clinical Study: Basic Fibroblast Growth Factor and Vascular Endothelial Growth Factor Levels

Serum samples were collected after 633 nm diode laser LLLT on 60 patients with complicated wounds. All blood samples were obtained after informed consent was provided. Immediately after venipuncture, peripheral blood was processed through centrifugation at 1500× *g* for 10 min. The basic fibroblast growth factor (bFGF) and vascular endothelial growth factor (VEGF) levels in the serum were measured using a commercially available kit (QIA55; Merck & Co., Inc., Whitehouse Station, NJ, USA). Using ELISA and monoclonal human anti-bFGF and anti-VEGF, bFGF and VEGF were detected with a high sensitivity alkaline phosphatase amplification system and horseradish peroxidase detection system, respectively (R&D Systems Inc., Minneapolis, MN, USA). Detectable concentration ranges were as follows: bFGF, 1–64 pg/mL for the high sensitivity assay and 9.97–640 pg/mL for the conventional assay; VEGF, 31.2–2000 pg/mL.

2.7. Statistical Analysis

We used SPSS 15.0 for Windows (SPSS, Chicago, IL, USA) for all data analyses. The data were presented in the form of means and standard deviations. The randomized block analysis of variance was used to determine whether the means of all four human fibroblast cell groups were equal. The possibility of inequality of variances across groups was analyzed using Levene's test [18]. While the assumption of equal variance was rejected, Welch's approach for correcting the F statistic of the analysis of variance was used. When the four means revealed a statistically significant difference, multiple comparisons of the means of any two groups were made using the least significant difference of the Games–Howell method. Differences in means were regarded as statistically significant with a two-tailed *p* value of <0.05. The amount of cell proliferation was compared among both groups before and after LLLT using the paired *t*-test. The same calculation was performed using the optical density of LDH and fibroblast-mediated type-I procollagen production for comparison. All data were presented as the mean ± standard deviation (SD).

3. Results

3.1. In Vitro Study: Human Fibroblast Cells

Fibroblast cell cultures were treated. A diode laser was applied to an area of 0.196 cm^2 with the three wavelengths of 633, 520, and 450 nm emitted separately. LLLT was administered with an irradiance of 3 mW/cm^2, where all three applications covered an area of 18 cm^2. In this experiment, laser exposure times are 0, 5, 15, and 45 min, where the HS68

cells are treated with a definitive fluence of LLLT irradiation. Therefore, HS68 cells can be operated in the absence (control) and presence of LLLT with fluences of 0.9, 2.7, and 8.1 J/cm^2, respectively. Microscopic findings showed high proliferation (Figure 2A–D) and cell viability of fibroblast cells in the 633 nm illuminated group. No statistically significant difference was observed between red light versus green and blue light in the viability analysis, as shown in Figure 3.
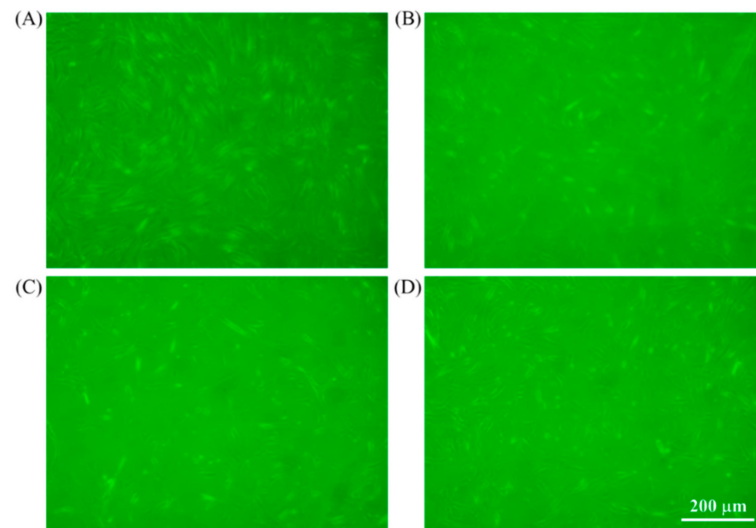

Figure 2. Microscopic findings (10×) demonstrated the proliferation of human fibroblast cells for (**A**) 633 nm, (**B**) 520 nm, and (**C**) 450 nm illumination and (**D**) control groups.
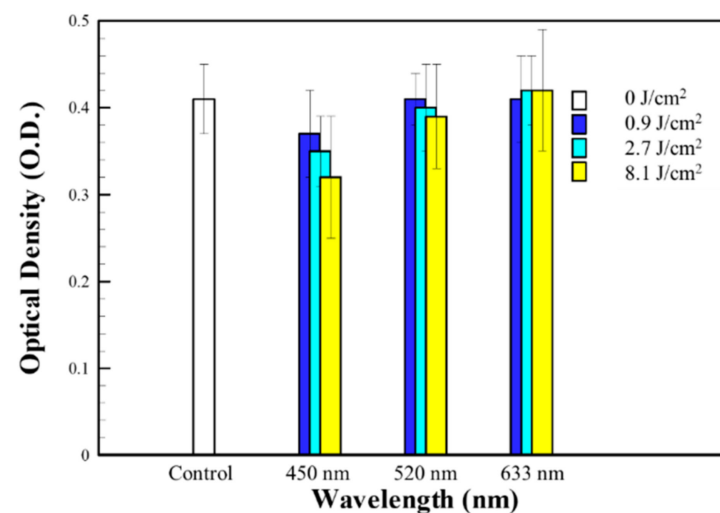

Figure 3. Viability assay of human fibroblast cells in the absence of LLLT (control group) and after LLLT with fluences of 0.9, 2.7, and 8.1 J/cm^2 at 450, 520, and 633 nm, respectively.

*3.2. In Vitro Study: Real-Time Polymerase Chain Reaction and Enzyme-Linked Immunosorbent Assay*

Statistical analysis of the percentage of fibroblast-mediated type-I procollagen production demonstrated a significant difference in the 633 nm group (40%) versus the 520 nm group (5%) and 450 nm group (2%) ($p < 0.05$). Furthermore, in RT-PCR, a significant difference in the relative expression of MMP-1, -2, and -9 was observed in the 633 nm group versus the 520 nm group and 450 nm group ($p < 0.05$). Therefore, the effects of LLLT on the cell cultures of fibroblast cells in vitro demonstrated a decrease in the relative expression of MMP-1, -2, and -9 while using light with a wavelength of 633 nm (Table 1).

Table 1. Comparison of relative expression of MMP-1, -2, and -9 under illumination at different wavelengths.

	MMP-1	MMP-2	MMP-9
Wavelength (nm)	**Mean ± SD (%)**		
Control	0.68 ± 0.13	0.67 ± 0.14	0.69 ± 0.02
633	0.13 ± 0.06	0.13 ± 0.07	0.15 ± 0.05
520	0.37 ± 0.11	0.30 ± 0.15	0.39 ± 0.09
450	0.41 ± 0.12	0.36 ± 0.11	0.45 ± 0.15

3.3. Clinical Study

Of the 60 patients, 42 were male and 18 were female, and their ages ranged from 38 to 71 years (mean, 51 years). All patients attained significant improvement with treatment (Figure 4A–C). The tissue biopsy slides from five wound sites were assessed through densitometric analysis using image analysis software (Leica Qwin V3 and Veica Microsystems CMS GmbH, Wetzlar, Germany). Under the fluorescence microscope, patients who received 633 nm red light illumination showed a concomitant increase in fibroblast collagen type I production (Figure 5A,B). The ranges of serum bFGF and VEGF levels before LLLT were 2.1–10.5 pg/mL (median 4.9) and 39–150 pg/mL (median 91.1), respectively. The ranges of serum bFGF and VEGF levels after 633 nm LLLT were 14.5–30.9 pg/mL (median 25.9) and 193–250 pg/mL (median 201.8), respectively. Significantly elevated bFGF and VEGF levels indicated their critical roles in wound healing ($p < 0.05$).

Figure 4. (**A**) A complicated wound of the right foot significantly improved with treatment (**B**) after 633 nm LLLT in 4 weeks, and (**C**) the final result was observed in 6 months.
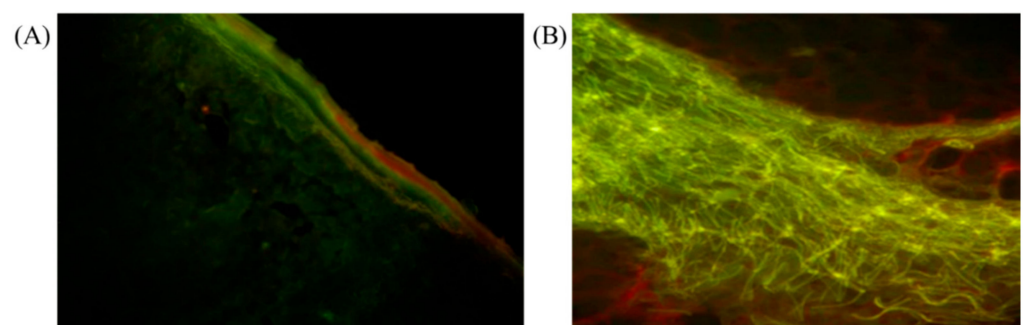
Figure 5. Under a fluorescent microscope, patients who received 633 nm red light illumination have a concomitant increase in fibroblast collagen type I production before (**A**) and after 633 nm LLLT in 6 months (**B**).

4. Discussion

Fibroblasts play an important role in cell therapy and tissue repair [19–21]. Proteoglycan, elastin, and other matrix proteins are produced by fibroblasts [22]. However, it is also critical that these cells express MMPs that damage collagen [23–28]. The epidermal and dermal cells degrade proteins to produce MMP enzymes, which then activate the enzymes that degrade the collagen that connects cells in the dermis [27]. As a result, MMPs are

crucial in the physiological mechanisms of wound healing. In our study, one of the most important mechanisms of fibroblasts was MMP expression. Despite numerous studies on a wide range of MMPs, the functional relevance of each MMP is unknown, and the associations between MMPs remain unclear [6,21–23,29]. However, activated MMP-1, a member of the collagenase subfamily of MMPs, initiates collagen breakdown by cleaving type-I and type-III collagen, which are further degraded by MMP-2 and -9 [30]. To study various factors related to MMPs, we investigated MMP-1, -2, and -9, which are known as collagenases [25].

Our results did not show a significant difference between red light versus green and blue light in LDH for detecting cell viability. However, the increased collagen expression was higher in the red light (633 nm) group. Furthermore, the results showed that the expression of MMP-1, -2, and -9 was relatively decreased in the red light (633 nm) group versus the green (520 nm) and blue light (450 nm) groups. Hence, our in vitro study, where the dependence of wavelength on light penetration depth can be excluded, demonstrates the importance of wavelengths as a significant variable for LLLT treatment. We believe that both MMP-1, -2, and -9 and collagen are essential for wound healing. While fibroblasts activate collagen remodeling, MMPs may be the key. We confirmed that various factors influence wound healing through mechanisms different than just the simple activation of fibroblasts by using red light (633 nm). Therefore, the red light (633 nm) group expressed remarkable results in wound healing. This study also supports the finding that the red–infrared band had better wound-healing effects at the organism level [12].

Conversely, angiogenesis has been well characterized as one of the key steps in wound healing. Furthermore, the roles of bFGF and VEGF as angiogenic cytokines are well known. This pathophysiological principle has recently attracted intense interest in wound healing. Although bFGF is an essential angiogenic stimulator in the complex regulatory machinery that leads to neovascularization, other factors are involved in this process. In our clinical study, we found an association between increased VEGF and red light (633 nm) in wound healing. The stimulation of platelet activities might be a possible explanation [31].

Although changes in MMP-1, -2, and -9 can be found in our study, the functional relevance of each MMP is not well known, and the connection between MMPs is unclear [21]. Further verifying the role of MMPs and reconfirming the results is required, which is one of our study's limitations and a potential area for future research. Furthermore, the percentage of human fibroblast cells killed by the optical density of the CytoTox 96^{TM} assay was calculated to monitor the results after LLLT. This method of defining the mechanisms of LLLT action has allowed us to design additional studies. Therefore, a variety of additional studies can be conducted based on our findings. The administration of LLLT to human fibroblast cells could play a vital role in wound care distinct from biological dressing materials.

5. Conclusions

Cultured fibroblasts likely play a crucial role in wound healing through different mechanisms. In our in vitro study, a significant decrease in the relative expression of MMP-1, -2, and -9 was observed in the 633 nm group versus the 520 nm group and 450 nm group. In addition, in our clinical study, 633 nm diode laser LLLT was only administered to patients with complicated wounds. Indeed, patients who received 633 nm red light illumination have a concomitant increase in fibroblast collagen type I production after 633 nm LLLT, which implies that red light (633 nm) activated collagen production and remodeling. Our studies indicated that LLLT might affect fibroblast cell growth processes involved in wound healing. The data derived from this study shall serve as the foundation for further clinical application. We anticipate that the proposed LLLT illumination system with multiple different wavelengths of diode lasers could be applied to construct innovative light prescriptions for photomedicine.

References

1. Chung, H.; Dai, T.; Sharma, S.K.; Huang, Y.Y.; Carroll, J.D.; Hamblin, M.R. The Nuts and Bolts of Low-level Laser (Light) Therapy. *Ann. Biomed. Eng.* **2012**, *40*, 516–533. [CrossRef] [PubMed]
2. De Freitas, L.F.; Hamblin, M.R. Proposed Mechanisms of Photobiomodulation or Low-Level Light Therapy. *IEEE J. Sel. Top. Quantum Electron.* **2016**, *22*, 7000417. [CrossRef] [PubMed]
3. Whelan, H.T.; Smits Jr, R.L.; Buchman, E.V.; Whelan, N.T.; Turner, S.G.; Margolis, D.A.; Cevenini, V.; Stinson, H.; Ignatius, R.; Martin, T. Effect of NASA light-emitting diode irradiation on wound healing. *J. Clin. Laser Med. Surg.* **2001**, *19*, 305–314. [CrossRef] [PubMed]
4. Whelan, H.T.; Wong-Riley, M.T.; Eells, J.T.; VerHoeve, J.N.; Das, R.; Jett, M. DARPA soldier self-care: Rapid healing of laser eye injuries with light emitting diode technology. In Proceedings of the RTO HFM Symposium on "Combat Casualty Care in Ground Based Tactical Situations: Trauma Technology and Emergency Medical Procedures", St. Pete Beach, FL, USA, 16–18 August 2004.
5. Whelan, H.T.; Buchmann, E.V.; Dhokalia, A.; Kane, M.P.; Whelan, N.T.; Wong-Riley, M.T.T.; Eells, J.T.; Gould, L.J.; Hammamieh, R.; Das, R.; et al. Effect of NASA light-emitting diode irradiation on molecular changes for wound healing in diabetic mice. *J. Clin. Laser Med. Surg.* **2003**, *21*, 67–74. [CrossRef]
6. Desmet, K.D.; Paz, D.A.; Corry, J.J.; Eells, J.T.; Wong-Riley, M.T.; Henry, M.M.; Buchmann, E.V.; Connelly, M.P.; Dovi, J.V.; Liang, H.L.; et al. Clinical and experimental applications of NIR-LED photobiomodulation. *Photomed. Laser Ther.* **2006**, *24*, 121–128. [CrossRef]
7. Mester, A.F.; Mester, A. Wound healing. *Laser Ther.* **1989**, *1*, 7–15. [CrossRef]
8. Trelles, M.A.; Allones, I. Red light-emitting diode (LED) therapy accelerates wound healing post-blepharoplasty and periocular laser ablative resurfacing. *J. Cosmet. Laser Ther.* **2006**, *8*, 39–42. [CrossRef]
9. Dall Agnol, M.A.; Nicolau, R.A.; de Lima, C.J.; Munin, E. Comparative analysis of coherent light action (laser) versus non-coherent light (light-emitting diode) for tissue repair in diabetic rats. *Lasers Med. Sci.* **2009**, *24*, 909–916. [CrossRef]
10. Corazza, A.V.; Jorge, J.; Kurachi, C.; Bagnato, V.S. Photobiomodulation on the angiogenesis of skin wounds in rats using different light sources. *Photomed. Laser Surg.* **2007**, *25*, 102–106. [CrossRef]
11. Erdle, B.J.; Brouxhon, S.; Kaplan, M.; Vanbuskirk, J.; Pentland, A.P. Effects of continuous-wave (670-nm) red light on wound healing. *Dermatol. Surg.* **2008**, *34*, 320–325.
12. Chen, Q.; Yang, J.; Yin, H.; Li, Y.; Qiu, H.; Gu, Y.; Yang, H.; Xiaoxi, D.; Xiafei, S.; Che, B.; et al. Optimization of photo-biomodulation therapy for wound healing of diabetic foot ulcers in vitro and in vivo. *Biomed. Opt. Express* **2022**, *13*, 2450–2466. [CrossRef] [PubMed]
13. Hopkins, J.T.; McLoda, T.A.; Seegmiller, J.G.; Baxter, G.D. Low-level laser therapy facilites superficial wound healing in humans: A triple-blind, sham-controlled study. *J. Athl. Train.* **2004**, *39*, 223–229. [PubMed]
14. Huang, C.-F.; Colley, M.M.S.; Lu, L.-S.; Chang, C.-Y.; Peng, P.-W.; Yang, T.-S. Performance characterization of continuous-wave laser-induced forward transfer of liquid bioink. *Appl. Phys. Express* **2019**, *12*, 116504. [CrossRef]
15. Pan, L.-C.; Hang, N.-L.; Colley, M.M.; Chang, J.; Hsiao, Y.-C.; Lu, L.-S.; Li, B.-S.; Chang, C.-J.; Yang, T.-S. Single Cell Effects of Photobiomodulation on Mitochondrial Membrane Potential and Reactive Oxygen Species Production in Human Adipose Mesenchymal Stem Cells. *Cells* **2022**, *11*, 972. [CrossRef] [PubMed]
16. Zuk, P.A.; Zhu, M.I.; Mizuno, H.; Huang, J.; Futrell, J.W.; Katz, A.J.; Benhaim, P.; Lorenz, H.P.; Hedrick, M.H. Multilineage Cells from Human Adipose Tissue: Implications for Cell-Based Therapies. *Tissue Eng.* **2001**, *7*, 211–228. [CrossRef]
17. Roberts, W.G.; Berns, M.W. In vitro photosensitation I. Cellular uptake and subcellular location of mono-L-aspartyl chlorin e6, chloro-aluminium sulfonated phthalocyanine, and photofrin®. *Lasers Surg. Med.* **1989**, *9*, 90–101. [CrossRef] [PubMed]

18. Lu, F.; Li, J.; Gao, J.; Ogawa, R.; Ou, C.; Yang, B.; Fu, B. Improvement of the Survival of Human Autologous Fat Transplantation by Using VEGF-Transfected Adipose-Derived Stem Cells. *Plast. Reconstr. Surg.* **2009**, *124*, 1437–1446. [CrossRef]

19. Kim, W.-S.; Park, B.-S.; Park, S.-H.; Kim, H.-K.; Sung, J.-H. Antiwrinkle effect of adipose-derived stem cell: Activation of dermal fibroblast by secretory factors. *J. Dermatol. Sci.* **2009**, *53*, 96–102. [CrossRef]

20. Kim, W.-S.; Park, B.-S.; Sung, J.-H. Protective role of adipose-derived stem cells and their soluble factors in photoaging. *Arch. Dermatol. Res.* **2009**, *301*, 329–336. [CrossRef]

21. Jeong, J.H.; Fan, Y.; You, G.Y.; Choi, T.H.; Kim, S. Improvement of photoaged skin wrinkles with cultured human fibroblasts and adipose-derived stem cells: A comparative study. *J. Plast. Reconstr. Aesthetic Surg.* **2015**, *68*, 372–381. [CrossRef]

22. Poulalhon, N.; Farge, D.; Roos, N.; Tacheau, C.; Neuzillet, C.; Michel, L.; Mauviel, A.; Verrecchia, F. Modulation of collagen and MMP-1 gene expression in fibroblasts by the immuno-suppressive drug rapamycin. A direct role as an antifibrotic agent? *J. Biol. Chem.* **2006**, *281*, 33045–33052. [CrossRef] [PubMed]

23. Kajanne, R.; Miettinen, P.; Mehlem, A.; Leivonen, S.-K.; Birrer, M.; Foschi, M.; Kähäri, V.-M.; Leppä, S. EGF-R regulates MMP function in fibroblasts through MAPK and AP-1 pathways. *J. Cell. Physiol.* **2007**, *212*, 489–497. [CrossRef] [PubMed]

24. Westermarck, J.; Holmström, T.; Ahonen, M.; Eriksson, J.E.; Kahari, V.M. Enhancement of fibroblast collagenase-1 (MMP-1) gene expression by tumor promoter okadaic acid is mediated by stress-activated protein kinases Jun N-terminal kinase and p38. *Matrix Biol.* **1998**, *17*, 547–557. [CrossRef]

25. Khoramizadeh, M.R.; Falak, R.; Pezeshki, M.; Ghahary, A.; Saadat, F.; Varshokar, K.; Safavifar, F.; Mansouri, P. Dermal wound fibroblasts and matrix metalloproteinases (MMPs): Their possible role in allergic contact dermatitis. *Iran. J. Allergy Asthma Immunol.* **2004**, *3*, 7–11.

26. Hattori, N.; Mochizuki, S.; Kishi, K.; Nakajima, T.; Takaishi, H.; D'Armiento, J.; Okada, Y. MMP-13 Plays a Role in Keratinocyte Migration, Angiogenesis, and Contraction in Mouse Skin Wound Healing. *Am. J. Pathol.* **2009**, *175*, 533–546. [CrossRef]

27. Howard, E.W.; Crider, B.J.; Updike, D.L.; Bullen, E.C.; Parks, E.E.; Haaksma, C.J.; Sherry, D.M.; Tomasek, J.J. MMP-2 expression by fibroblasts is suppressed by the myofibroblast phenotype. *Exp. Cell Res.* **2012**, *318*, 1542–1553. [CrossRef]

28. Lindner, D.; Zietsch, C.; Becher, P.M.; Schulze, K.; Schultheiss, H.-P.; Tschöpe, C.; Westermann, D. Differential Expression of Matrix Metalloproteases in Human Fibroblasts with Different Origins. *Biochem. Res. Int.* **2012**, *2012*, 875742. [CrossRef]

29. Kim, J.-H.; Jung, M.; Kim, H.-S.; Kim, Y.-M.; Choi, E.-H. Adipose-derived stem cells as a new therapeutic modality for ageing skin. *Exp. Dermatol.* **2011**, *20*, 383–387. [CrossRef]

30. Nagase, H.; Visse, R.; Murphy, G. Structure and function of matrix metalloproteinases and TIMPs. *Cardiovasc. Res.* **2006**, *69*, 562–573. [CrossRef]

31. Banks, R.; Forbes, M.A.; Kinsey, S.E.; Stanley, A.; Ingham, E.; Walters, C.; Selby, P.J. Release of the angiogenic cytokine vascular endothelial growth factor (VEGF) from platelets: Significance for VEGF measurements and cancer biology. *Br. J. Cancer* **1998**, *77*, 956–964. [CrossRef]